Title

Climate and plant trait strategies determine tree carbon allocation to leaves and mediate future forest productivity

Journal

Global Change Biology, 25(10)

ISSN

1354-1013

Authors

Trugman, Anna T
Anderegg, Leander DL
Wolfe, Brett T
et al.

Publication Date

2019-10-01

DOI

10.1111/gcb.14680

Peer reviewed

Received: 19 December 2018 | Revised: 2 May 2019 | Accepted: 4 May 2019

DOI: 10.1111/gcb.14680

PRIMARY RESEARCH ARTICLE

Global Change Biology WILEY

Climate and plant trait strategies determine tree carbon allocation to leaves and mediate future forest productivity

Anna T. Trugman[1,2] | Leander D. L. Anderegg[3,4] | Brett T. Wolfe[5] | Benjamin Birami[6] | Nadine K. Ruehr[6] | Matteo Detto[7] | Megan K. Bartlett[7,8] | William R. L. Anderegg[1]

[1]School of Biological Sciences, University of Utah, Salt Lake City, Utah

[2]Department of Geography, University of California, Santa, Santa Barbara, California

[3]Department of Global Ecology, Carnegie Institution for Science, Stanford, California

[4]Department of Integrative Biology, University of California, Berkeley, Berkeley, California

[5]Smithsonian Tropical Research Institute, Balboa, Panama

[6]Institute of Meteorology and Climate Research – Atmospheric Environmental Research (IMK-IFU), Karlsruhe Institute of Technology (KIT), Garmisch-Partenkirchen, Germany

[7]Department of Ecology and Evolutionary Biology, Princeton University, Princeton, New Jersey

[8]Department of Viticulture and Enology, University of California, Davis, California

Correspondence
Anna T. Trugman, School of Biological Sciences, University of Utah, Salt Lake City, UT 84112, USA.
Email: a.trugman@utah.edu

Funding information
USDA National Institute of Food and Agriculture, Grant/Award Number: 2018-67012-28020 and 2018-67019-27850; National Science Foundation, Grant/Award Number: 1714972 and 1802880; German Research Foundation, Grant/Award Number: RU 1657/2-1, SCHM 2736/2-1 and YA 274/1-1 ; David and Lucille Packard Foundation; University of Utah Global Change and Sustainability Center; Next-Generation Ecosystem Experiments-Tropics; Biological and Environmental Research; German Federal Ministry of Education and Research; Helmholtz Association

Abstract

Forest leaf area has enormous leverage on the carbon cycle because it mediates both forest productivity and resilience to climate extremes. Despite widespread evidence that trees are capable of adjusting to changes in environment across both space and time through modifying carbon allocation to leaves, many vegetation models use fixed carbon allocation schemes independent of environment, which introduces large uncertainties into predictions of future forest responses to atmospheric CO_2 fertilization and anthropogenic climate change. Here, we develop an optimization-based model, whereby tree carbon allocation to leaves is an emergent property of environment and plant hydraulic traits. Using a combination of meta-analysis, observational datasets, and model predictions, we find strong evidence that optimal hydraulic–carbon coupling explains observed patterns in leaf allocation across large environmental and CO_2 concentration gradients. Furthermore, testing the sensitivity of leaf allocation strategy to a diversity in hydraulic and economic spectrum physiological traits, we show that plant hydraulic traits in particular have an enormous impact on the global change response of forest leaf area. Our results provide a rigorous theoretical underpinning for improving carbon cycle predictions through advancing model predictions of leaf area, and underscore that tree-level carbon allocation to leaves should be derived from first principles using mechanistic plant hydraulic processes in the next generation of vegetation models.

KEYWORDS
aridity gradient, carbon allocation, climate change, CO_2 fertilization, leaf area, plant hydraulic traits, sapwood area, vegetation model

1 | INTRODUCTION

Forest leaf area mediates both terrestrial ecosystem productivity and drought-driven tree mortality during climate extremes (Jump et al., 2017; Myneni et al., 2001; Nemani et al., 2003; Zhu et al., 2016). Tree allocation to leaf area is fundamental to forest climate responses because the water lost through the canopy cannot exceed the water supplied by the sapwood (tree water

transport tissue), thus the ratio of plant leaf area (A_L) to sapwood area (A_S) constrains whole-plant photosynthesis (Sperry & Love, 2015). During climatic extremes, such as droughts, the increased evaporative demand of the forest canopy relative to supply capacity of the sapwood drives plants to reduce transpiration through stomatal closure to avoid strong tensions and hydraulic failure in the xylem, which can induce metabolic stress, hydraulic damage, and even mortality (Jump et al., 2017; Martinez-Vilalta et al., 2009; Trugman et al., 2018). Thus, the optimal canopy (i.e., tree leaf area) for a tree to support, or the A_L:A_S ratio that maximizes net primary productivity (NPP) (commonly used as a proxy for plant fitness; Franklin et al., 2012), is dependent on local water availability and atmospheric conditions.

Coordination of tree leaf and sapwood area has been observed to be a major physiological mechanism through which trees adjust to changes in water availability and moderate internal plant water stress (Carter & White, 2009; Rosas et al., 2019). Within species, A_L:A_S exhibits greater plasticity across environmental gradients than other common physiological traits that are important for predicting tree water stress, such as the water potential at which 50% loss of stem hydraulic conductance occurs (P50; Rosas et al., 2019). Observations of coordinated leaf area adjustment with water availability have been extensively documented across plant physiological scales and environmental gradients ranging from hydraulic adjustment of A_L:A_S at the branch- or tree-level (DeLucia, Maherali, & Carey, 2000; Martinez-Vilalta et al., 2009; Mencuccini & Bonosi, 2001; Mencuccini & Grace, 1994; Pinol & Sala, 2000; Rosas et al., 2019), to ecosystem-level trends in forest leaf area due to regional differences in water availability (Baldocchi & Xu, 2007; Eagleson, 1982; Gholz, 1982; Joffre & Ramball, 1993). Importantly, trees are responsive to changes in water supply not just over space but also over annual-scale time periods through changes in both the rate of leaf production and leaf turnover, mechanisms through which trees decrease A_L:A_S with increasing water stress (Limousin et al., 2012).

The concepts of acclimation and adaptation of A_L:A_S to changing climate conditions are crucial when considering future forest productivity because anthropogenic climate change has a strong potential to alter tree allocation to A_L:A_S and forest leaf area, which greatly impact terrestrial ecosystem productivity. However, the sum of the effects of different climate change drivers is unclear. For example, projected increases in atmospheric vapor pressure deficit (VPD) with warmer temperatures (Williams et al., 2012) have the potential to drive decreases in A_L:A_S and forest leaf area. In contrast, increases in plant water use efficiency associated with higher concentrations of atmospheric CO_2 may increase the amount of leaf area that forest ecosystems can support under a fixed climatic water supply. Thus, anticipating future forest carbon allocation and terrestrial productivity requires a better understanding of how leaf area adjustment is mediated by plant and environmental factors, including the role of physiological traits that are important to plant water stress (e.g., P50), and the net effect of VPD and CO_2 fertilization as competing environmental drivers.

Here, we used observational data of hydraulic adjustment of A_L:A_S across environmental gradients, a meta-analysis of the CO_2 fertilization literature documenting adjustment of A_L:A_S, and an optimization-based model of tree gas exchange, hydraulic transport, and carbon allocation (Figure S1; Trugman et al., 2018) to ask: (a) Do geographic patterns of A_L:A_S within- and across species match optimality-based predictions? (b) What environmental factors are most important to variability in A_L:A_S? (c) What physiological drivers or functional traits are responsible for variability in A_L:A_S? (d) Which functional traits are most important for understanding regional trends in A_L:A_S in response to global environmental change?

2 | MATERIALS AND METHODS

2.1 | Measured response of A_L:A_S across a climate gradient in Western Australia and Tasmania

We measured A_L:A_S for terminal twigs (cut at the first branching point) for one Acacia and seven different Eucalyptus species (*Acacia acuminata*, *Eucalyptus amygdalina*, *Corymbia calophylla*, *Eucalyptus marginata*, *Eucalyptus salmonophoia*, *Eucalyptus obliqua*, *Eucalyptus ovata*, *Eucalyptus viminalis*) across a large aridity gradient (Midsummer (January) VPD ranging from 460 Pa to 2,460 Pa) in Western Australia and Tasmania in October 2014 and February 2016, respectively. For each species, we collected samples from four to five sites, covering as much of their aridity range as possible. Each site comprised of three plots that were located >500 m but generally <5 km apart. At each plot, average A_L:A_S was calculated for five trees based on three branch samples per tree from the sun exposed, north-facing canopy. We looked at how A_L:A_S varied with January VPD using plot location and ~0.86 km^2 resolution monthly climate data from the WorldClim Global Climate Data (Fick & Hijmans, 2017).

2.2 | Measured response of A_L:A_S in Panamanian seasonally dry tropical forests

Observational measurements for six species with distinct traits and drought phenologies of seasonal leaf area were conducted in two seasonally dry forests in Panama, the Parque Natural Metropolitano (8°59′N, 79°32′W) with annual rainfall of 1,800 mm, and the Eugene Eisenmann Reserve (8°31′N, 79°53′W) with annual rainfall of 1,590 mm (Wolfe, Sperry, & Kursar, 2016). Both are mature secondary forests that experience dry seasons from mid-December to May. Tree species and phenology type included in this study are as follows: *Annona hayesii* (brevi-deciduous), *Genipa americana* (deciduous), *Bursera simaruba* (deciduous), *Cavanillesia platanifolia* (deciduous), *Cojoba rufescens* (evergreen), *Astronium graveolens* (evergreen). Full methodological details regarding observational data collection are available from Wolfe et al. (2016).

2.3 | Literature search for the A_L:A_S response to CO_2

We compiled data drawing from two meta-analyses of CO_2 fertilization experiments (Ainsworth & Long, 2005; Gielen & Ceulemans,

2001), a Google Scholar search of studies documenting the impacts of CO_2 fertilization on woody species, and a CO_2 fertilization experiment of *Pinus halepensis* (Supplementary Methods). Studies that satisfied the following constraints were included: (a) Woody species were included in the experiment; (b) some metric analogous to sapwood area (including basal area, tree diameter at breast height (dbh), or sapwood area) was recorded; and (c) some metric analogous to leaf area (including leaf biomass, LAI, or leaf area) was documented. These criteria rely on the following assumptions: (a) tree sapwood area is linearly related to tree basal area and the sapwood to basal area ratio is invariant with tree size (a simplification that is broadly consistent with reports in the literature; Meinzer, Goldstein, & Andrade, 2001), (b) leaf area is linearly related to leaf biomass (and this relationship is invariant with tree size), and (c) leaf area can be approximated by LAI. Although these approximations are imperfect, they are necessary given the limited number of studies that document changes in A_L:A_S with CO_2 fertilization. This led to the identification of 11 published studies in addition to our experiment using *Pinus halepensis* that span a CO_2 gradient of 360 ppm to 870 ppm for 19 different species derived from both field and closed chamber experiments on both seedlings and larger trees (Table S1).

We quantified the sensitivity of A_L:A_S to CO_2 using linear mixed effects models. We included ΔA_L:A_S as the response variable, ΔCO_2 as a fixed effect, and study as a random effect. We computed the relative change ΔA_L:A_S as

$$\Delta A_L{:}A_S = \frac{(A_L{:}A_S)_E - (A_L{:}A_S)_C}{(A_L{:}A_S)_C},$$

where "E" signifies A_L:A_S at elevated CO_2 and "C" signifies A_L:A_S at control CO_2 concentrations (both of which vary by study, Table S1). We experimented with including fixed effects to account for additional treatment type (nitrogen, water stress, ozone tolerance) and angiosperm versus gymnosperm classification, however, these fixed effects were not significant and increased the AIC, so we opted for the most parsimonious model relating ΔA_L:A_S to ΔCO_2 (Table S2). We then used results from our mixed effects model analysis to project ΔA_L:A_S with an approximate doubling of atmospheric CO_2 concentrations from 400 ppm to 800 ppm. Response coefficients in the mixed effects models were estimated using a maximum likelihood Laplace approximation with the *fitglme* function in MATLAB.

2.4 | Tree model

We use a simple tree model that couples plant hydraulics to photosynthetic carbon gain (the Hydraulic Optimization Theory for Tree and Ecosystem Resilience or HOTTER model). The HOTTER model uses a single resistor to represent whole-plant hydraulic transport up to the substomatal cavity and a hydraulic optimization-based stomatal conductance model (Trugman et al., 2018; Wolf, Anderegg, & Pacala, 2016). While the model contains some necessary simplifications, it is broadly consistent with the Ohm's law analogy for hydraulic elements in series and the observed responses of gas exchange to changes in leaf-specific hydraulic conductance (Hubbard, Ryan, Stiller, & Sperry, 2001; Sperry, 2000). HOTTER optimizes A_L:A_S to maximize NPP (Figure S1) given the following environmental inputs: VPD (a metric of atmospheric dryness), soil water content, and atmospheric CO_2 concentration. Tree biological parameters that influence whole-plant photosynthesis in HOTTER include hydraulic traits (maximum stem water conductivity, K_{max}, and P50), A_L:A_S, tree size, as well as a number of other physiological traits (Table S3). HOTTER assumes that photosynthesis is not significantly light or nutrient limited, all leaves experience the same VPD and CO_2, and all fine roots experience the same soil water potential. We provide a description of the HOTTER model below and a full derivation in the Supplementary Information.

Water transport within the soil/plant continuum is represented in HOTTER by the pipe model of a tree (Shinozaki, Yoda, Hozumi, & Kira, 1964). Flow from the soil to the plant roots, stem, and out of the stomata is driven by soil water potential and VPD, and it is regulated by plant physiological traits. Water storage within the plant is not represented, an assumption that recent work suggests is justified for reasonably long recovery timescales (Huang et al., 2017). The flow, F, throughout a plant element is computed by integrating the hydraulic conductivity per unit of xylem area (K) from one end of the pipe continuum with water potential ψ_1 to the other with water potential ψ_2 (Sperry, Adler, Campbell, & Comstock, 1998), which can be expressed by the differences in the Kirchhoff transforms as:

$$F = \frac{a}{L}\int_{\psi_1}^{\psi_2} K(\psi)\,d\psi = \frac{a}{L}(\phi_2 - \phi_1). \quad (1)$$

where a is the xylem area of the element and L the pipe length. The element conductivity (K) decreases as stem water potential falls as a result of embolism. A logistic function is used to represent the loss of conductivity as water potential becomes more negative.

Water flow from the roots to the stem, leaves, and into the atmosphere is modeled as

$$\frac{a_{root}}{L_{root}}(\phi_{soil} - \phi_{root}) = \frac{a_{stem}}{L_{stem}}(\phi_{root} - \phi_{stem}) = \frac{a_{petiole}}{L_{petiole}}(\phi_{stem} - \phi_{leaf}) = a_{leaf} g_s D, \quad (2)$$

where a_{root}, a_{stem}, $a_{petiole}$, and a_{leaf} are the surface area of the tree roots, cross-sectional area of the xylem, and cross-sectional xylem area within a given petiole summed over the tree, and leaf area, respectively. L_{root}, L_{stem}, and $L_{petiole}$ are the path length from the soil to the base of the stem, the tree height, and the length of the petiole, respectively. ϕ_{soil}, ϕ_{root}, ϕ_{stem}, and ϕ_{leaf} are the integral of the conductivity for the soil, roots, stem, and petiole, respectively, calculated from the Kirchhoff transform (Equation 1). g_s is stomatal conductance and D is the VPD. As a simplification, this formulation represents a tree canopy as comprised of a single leaf layer and assumes that under average growth conditions the two limiting photosynthetic rates (i.e., the photosynthetic rate limited by the maximum rate of Rubisco carboxylation and the photosynthetic rate limited by the electron transport rate for the regeneration of ribulose-1,5,-bisphosphate) should be equal according to Smith et al. (2019).

Stomatal conductance, g_s, is modeled following a modified version of the Leuning model that incorporates the effect of soil water potential on plant leaf water potential (Leuning, 1995; Wolf et al., 2016),

$$x_c = \frac{g_s}{A_n} = \frac{c_1}{(C_a - \Gamma)\left(1 + \frac{D}{D_0}\right)} \beta(\psi_L). \quad (3)$$

In Equation 3, C_a is the atmospheric CO_2 concentration, c_1, D_0, and Γ are empirical constants from the Leuning model (Table S3), A_n is net photosynthesis, ψ_L is leaf water potential. The function β represents the stomatal response to leaf water potential and serves to downregulate photosynthesis under water-stressed conditions. The β function is determined by the carbon cost of sustaining negative water potential and loss of conductivity in the stem. For simplicity we assumed that β increases linearly with the integral of the conductivity of the petiole from the Kirchhoff transform

$$\beta = \frac{\phi_{leaf}}{\phi_{max}}, \quad (4)$$

where ϕ_{max} is the integral of maximum hydraulic conductivity of the xylem (Table S3). β varies between 1 (leaf at full hydration) and 0 (leaf under full water stress) and captures the monotonic decrease in β with more negative leaf water potentials (Wolf et al., 2016). Here, β broadly conforms to the solution for the Leuning model, but with a more mechanistic representation of soil moisture stress through soil water potential's effect on leaf water potential.

We assume the classic photosynthetic model of CO_2 demand (Farquhar, Caemmerer, & Berry, 1980),

$$A_n = V'_{c,max} \frac{C_i - \Gamma^*}{C_i - k_m} - R. \quad (5)$$

In Equation 5, C_i is the interstitial CO_2 concentration, R is the daytime leaf respiration, $V'_{c,max}$ is an estimate of the effect of absorbed light on maximum rate of carboxylation based on the assumption that the electron transport and Rubisco-limited rates of photosynthesis are colimiting under typical daytime conditions (Smith et al., 2019; Wang et al., 2017; Supplementary Methods), Γ^* is the CO_2 compensation point in the absence of mitochondrial respiration, and k_m is the Michaelis constant (ppm) for the Farquhar model (Farquhar et al., 1980). We rewrite Fick's Law for diffusion of CO_2 from the atmosphere through the stomata in terms of x_c using Equation 3 as

$$C_i = \left(C_a - \frac{1}{x_c}\right). \quad (6)$$

Given the solution for x_c and the expression for photosynthesis in terms of x_c (see full derivation in the Supplementary Information), we relate A_n to tree size, functional leaf and xylem biomass, and hydrological and atmospheric drivers. Finally, we calculate NPP for the whole plant (including all respiration costs) as

$$NPP = (1 - \varepsilon)(A_n - R_{root} - R_{phloem} - R_{xylem} - R_{dark}). \quad (7)$$

In Equation 7, NPP includes growth and maintenance respiration costs, ε is the growth respiration fraction, R_{root} is the root respiration, R_{phloem} is the combined respiration rate of the phloem and cambium (which remains proportional to tree size regardless of drought-induced hydraulic damage to the xylem), R_{xylem} is the respiration rate of the xylem (which is proportional to functional xylem biomass and decreases with decreased functional xylem resulting from drought-induced hydraulic damage), and R_{dark} is the dark respiration rate of the leaves. Although growth respiration can vary appreciably with age (Mäkelä & Valentine, 2001), we treat it as constant in the interest of parsimony and in accordance with a number of other widely utilized vegetation models (Medvigy, Wofsy, Munger, Hollinger, & Moorcroft, 2009).

2.5 | HOTTER Model predictions for the A_L:A_S response to environmental conditions

We compared trends in model-predicted A_L:A_S that maximized NPP (Figure S1) along an atmospheric moisture gradient to observed trends in A_L:A_S across Western Australia and Tasmania. HOTTER plant traits were representative of Australian species (Table S3 note). Atmospheric CO_2 (=400 ppm) and soil water potential (=−1 MPa) were kept constant (due to a lack of site-specific soil moisture data). We varied VPD across environmentally relevant values ranging from 500 Pa to 2,500 Pa. In this comparison, we assumed that plants behave as pipe models such that the A_L:A_S is conserved along the height of the tree (Shinozaki et al., 1964). Although a better understanding of A_L:A_S variability within trees would allow for more rigorous scaling techniques from branch-level measurements to trees, data are currently limiting, and a number of studies suggest that our scaling assumption is reasonable (Mencuccini, Manzoni, & Christoffersen, 2018).

Next, we compared measurements of observed leaf area for six species with distinct traits and drought phenologies documented by Wolfe et al. (2016) with model-predicted optimal leaf areas that maximized NPP, given site-specific climate and species-specific hydraulic and photosynthesis traits (Figure S2, Table S4). Climate data used to force HOTTER were derived from site-specific daily mean VPD. We applied a smoothing low-pass filter to VPD spanning 10% of the measurement period to avoid the impacts of daily variability in VPD because we were interested in capturing the effects of seasonal trends in water availability on predicted changes in A_L. Site-specific soil moisture data were not available. However, predawn leaf water potentials are generally representative of soil water potentials and were measured by Wolfe et al. (2016). Thus, we reconstructed soil moisture by gap-filling mean predawn leaf water potential measurements at each site across all species except for *Bursera simaruba* and *Cavanillesia platanifolia* (which disconnect from the soil before the soil dries, and so do not necessarily have predawn leaf water potentials that are representative of the soil water content; Wolfe, 2017) to obtain daily-level soil moisture forcing datasets for HOTTER model predictions for both the Parque Natural Metropolitano and the Eugene Eisenmann Reserve. Because measurements for canopy CO_2 were

not available, we assumed a constant CO_2 = 400 ppm. Model predictions of the seasonal dynamics of relative A_L (calculated as current A_L relative to maximum A_L during the 2011–2013 measurement period) given site-specific climate and species-specific traits were compared to observed seasonal dynamics of relative A_L for each species at each site.

Finally, we used HOTTER to predict trends in A_L:A_S that maximized NPP along a CO_2 gradient ranging from preindustrial levels (280 ppm) to an approximate doubling of current CO_2 concentrations (800 ppm). We assumed an 8% depression in SLA for trees exposed to elevated CO_2 concentrations in accordance with Ainsworth and Long (2005). All other plant traits (Table S3), atmospheric VPD (=1,200 Pa), and soil water potential (=−1 MPa) were kept constant. We then compared the model-predicted sensitivity of A_L:A_S to the sensitivity of the meta-analysis observed A_L:A_S by projecting the change in A_L:A_S with a doubling in CO_2 concentrations from 400 ppm to 800 ppm using both the mixed effects model response coefficient (Table S2) and the HOTTER model.

2.6 | HOTTER estimates of the sensitivity of A_L:A_S to climate change and global variation in traits

To understand the sensitivity of A_L:A_S to changes in VPD and CO_2 with anthropogenic climate change, we ran factorial simulations forced with VPD, soil moisture, and atmospheric CO_2 concentrations. We derived model forcing from the Coupled Model Intercomparison Project Phase 5 (CMIP5) for the steepest CO_2 emissions scenario, the Representative Concentration Pathway (RCP) 8.5. We ran simulations using average climate conditions over historical (1981–2000) and future (2080–2099) climates (Figure S3). Factorial simulations were as follows: (a) historical soil moisture and VPD and globally constant CO_2 = 370 ppm; (b) historical soil moisture, constant CO_2 = 370 ppm, and RCP 8.5 projected VPD; (c) historical soil moisture and VPD and RCP 8.5 projected globally constant CO_2 = 925 ppm; and (d) RCP 8.5 projected soil moisture and VPD and globally constant CO_2 = 925 ppm. We found the soil moisture effect between historical and RCP 8.5 to be minimal compared to the VPD and CO_2 effects and thus did not include it in our analysis. We used the multimodel median soil water potential and atmospheric VPD to understand the sensitivity of the HOTTER model allocation predictions to predicted changes in mean climate (Figure S3). We assumed that tree size remained constant between current and future projections and initialized the model with the tree size dataset from Simard, Pinto, Fisher, & Baccini (2011). We converted tree height to dbh (required for the idealized tree model input) assuming the allometric relationship from Table S3. Overall, these simulations were designed to understand the sensitivity of A_L:A_S to mean changes in VPD and CO_2 rather than to predict absolute changes in forest leaf area globally, given assumptions of constant tree height and the lack of competition in the HOTTER model.

To understand the sensitivity of A_L:A_S to plant trait strategy and how trait strategy interacts with climate, we varied biome-specific traits globally including specific leaf area (SLA), maximum stem water conductivity (K_{max}), and P50 based on Anderegg, (2015) and Oleson et al. (2010) (Table S5). K_{max} was not included in these databases so we varied K_{max} proportionally with $V_{c,max}$. All other traits remained constant (Table S3). We then used a 0.5° resolution MODIS land cover map from year 2000 (http://glcf.umd.edu/data/lc/) upscaled to 1° for the purposes of determining grid cell-specific traits (Channan, Collins, & Emanuel, 2014; Friedl et al., 2010). We included all forest types in in our simulations with possible woody plant cover including Evergreen Needleleaf forest, Evergreen Broadleaf forest, Deciduous Needleleaf forest, Deciduous Broadleaf forest, Mixed forest, Closed shrubland, Open shrubland, Woody savanna, Savanna (code values 1–9). For grid cells of mixed forest type, we assumed each species type occupied 50% of the grid area and ran two simulations examining the sensitivity of A_L:A_S, one with each species trait type and took the average A_L:A_S prediction derived from these two simulations. We ran an additional set of five simulations, forced the model with RCP 8.5 projected VPD, soil moisture, and CO_2, to quantify the relative importance of SLA, $V_{c,max}$, K_{max}, and P50 in determining A_L:A_S. We held fixed one trait, either P50, SLA, $V_{c,max}$, or K_{max}, and varied all others. We then quantified the trait effect on ΔA_L:A_S by looking at the percent difference between the fixed trait simulation minus the globally varying trait simulation quantity divided by the globally varying trait simulation. These simulations were designed to understand the relative importance of different physiological traits on influencing tree A_L:A_S and to place this sensitivity in the context of spatial variation in global climate. Although many of these physiological traits covary in reality due to physiological trade-offs (and this covariation would impact the sensitivity of modeled A_L:A_S), this modeling analysis allowed us to isolate individual trait effects in a manner that would be impossible to do in the field.

3 | RESULTS

The optimality-based HOTTER model predicted a negative relationship between A_L:A_S and increased water stress (Figure 1a). Thus, given an expected atmospheric dryness or soil water availability, the optimal strategy for a tree is to decrease A_L:A_S as water availability decreases. Indeed, the HOTTER model captured the observed decrease in A_L:A_S and the rate of change in A_L:A_S with increasing VPD across a large climate gradient in Australia and Tasmania (ranging from 300 to 1,475 mm in mean annual precipitation and 460 to 2,460 Pa in midsummer VPD). As VPD increased, allocation to A_L relative to A_S decreased asymptotically. At low to moderate VPD levels, this corresponded to a rapid downregulation of A_L:A_S with increased VPD. However, the adjustment in A_L:A_S slowed at more extreme VPD stresses. Interestingly, substantial intraspecific variability in A_L:A_S existed in the observations at a fixed VPD that was not predicted by the HOTTER model, potentially due to a disconnect between VPD and soil water availability at different sites (Novick et al., 2016). Given a lack of site-specific soil moisture, it was not possible to test how access to groundwater impacted observed A_L:A_S responses or incorporate soil water

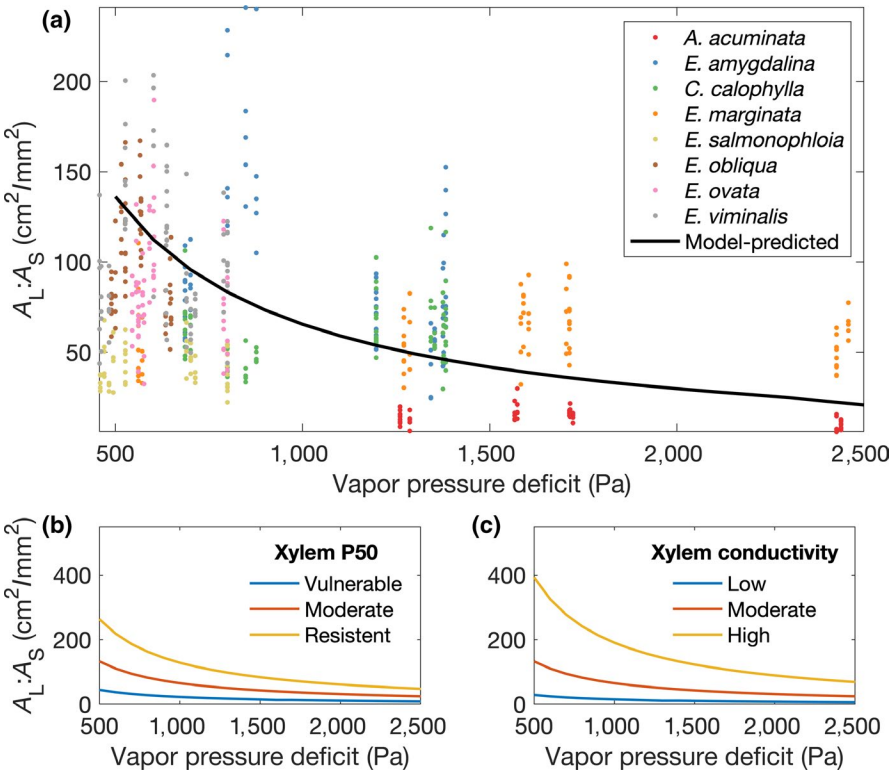

FIGURE 1 Observed and model-predicted inter- and intraspecific variability in structural allocation to leaf area relative to sapwood area (A_L:A_S) along an atmospheric vapor pressure deficit gradient in Western Australia and Tasmania. (a) Observed (colored points) and model-predicted (black line) allocation to A_L:A_S across a vapor pressure deficit gradient for eight different species including *Acacia acuminata* (red), *Eucalyptus amygdalina* (blue), *Corymbia calophylla* (green), *Eucalyptus marginata* (orange), *Eucalyptus salmonophoia* (yellow), *Eucalyptus obliqua* (brown), *Eucalyptus ovata* (pink), and *Eucalyptus viminalis* (grey). Model-predicted sensitivity of A_L:A_S to changes in (b) P50 (xylem resistance to negative water potentials) and (c) xylem conductivity

responses in HOTTER predictions. However, site-specific VPD alone was sufficient to predict broad allocational trends in A_L:A_S across species.

Plant hydraulic traits influenced the optimal A_L:A_S. Specifically, plants with a more resistant xylem, corresponding to a more negative P50, were able to support more leaf area and maintain photosynthesis at all VPD levels (Figure 1b). Similarly, plants with a high maximum stem water conductivity (K_{max}) were able to support more leaf area at all VPD levels (Figure 1c) because higher conductivities decreased internal water stress on plant tissues, provided sufficient soil water is available to maintain a higher conductivity. Although hydraulic traits were integral in predicting the optimal A_L:A_S with a given water availability, the A_L:A_S response to increasing VPD (i.e., the shape of the curve) was robust regardless of plant trait strategy (Figure 1b,c).

We then considered whether optimality theory could predict seasonal variations in A_L:A_S given intra-annual variations in environmental conditions. Seasonally dry tropical forests provide the ideal biome in which to test the model because plant hydraulic traits are informative of temporal variations in A_L:A_S (i.e., evergreen or deciduous phenological strategy). Indeed, when we compared the observed seasonal phenology of six different tropical dry forest tree species to HOTTER, parameterized with species-specific hydraulic traits and forced with observed daily-level VPD and soil moisture, the model predicted the phenology of drought deciduous trees (and to an extent the phenology of brevi-deciduous trees) by allocating to leaves to maximize NPP (Figure 2a–d). In contrast, HOTTER was not able to predict the seasonal leaf phenology of evergreen species. However, hydraulic traits alone were predictive of some leaf retention in the evergreen species (which are more tolerant to decreased water availability) during the dry season (Figure 2e,f), despite the lack of light-driven competition dynamics in HOTTER that are influential in tropical dry forest evergreen phenology.

In addition to water availability, A_L:A_S has been shown to be sensitive to increased atmospheric CO_2 concentrations (see Tables S1 and S2 for studies included in this meta-analysis) because high atmospheric CO_2 increases tree water use efficiency, potentially increasing A_L:A_S for a fixed climatic water availability. HOTTER predictions showed an increase in optimal A_L:A_S by ~70% with a doubling of CO_2 from 400 to 800 ppm, with all other climate conditions and plant traits held constant (Figure 3). We performed a meta-analysis of CO_2 fertilization studies derived from field and closed chamber experiments that are representative of both seedlings and larger trees and used mixed effects models to project ΔA_L:A_S with an approximate doubling of atmospheric CO_2 concentrations from 400 to 800 ppm. The model-predicted fertilization response fell well within the meta-analysis observed response range (Figure 3b; Tables S1 and S2).

Taken together, the optimal allocation model HOTTER appears to explain plant allocation patterns across both space—among and within species—and time and in response to the critical drivers of water availability and CO_2 concentrations. Thus, we applied HOTTER to understand the sensitivity of plant carbon allocation to both future climate conditions and physiological trait strategies. HOTTER predicted that the increased water use efficiency associated with strong atmospheric CO_2 fertilization will likely outweigh the increased water stress associated with predicted mean increases in VPD, resulting in a potential increase in A_L:A_S under mean climate conditions circa 2100 for most locations around the globe (Figure 4). Notable exceptions to this mean climate response included portions of Brazil in

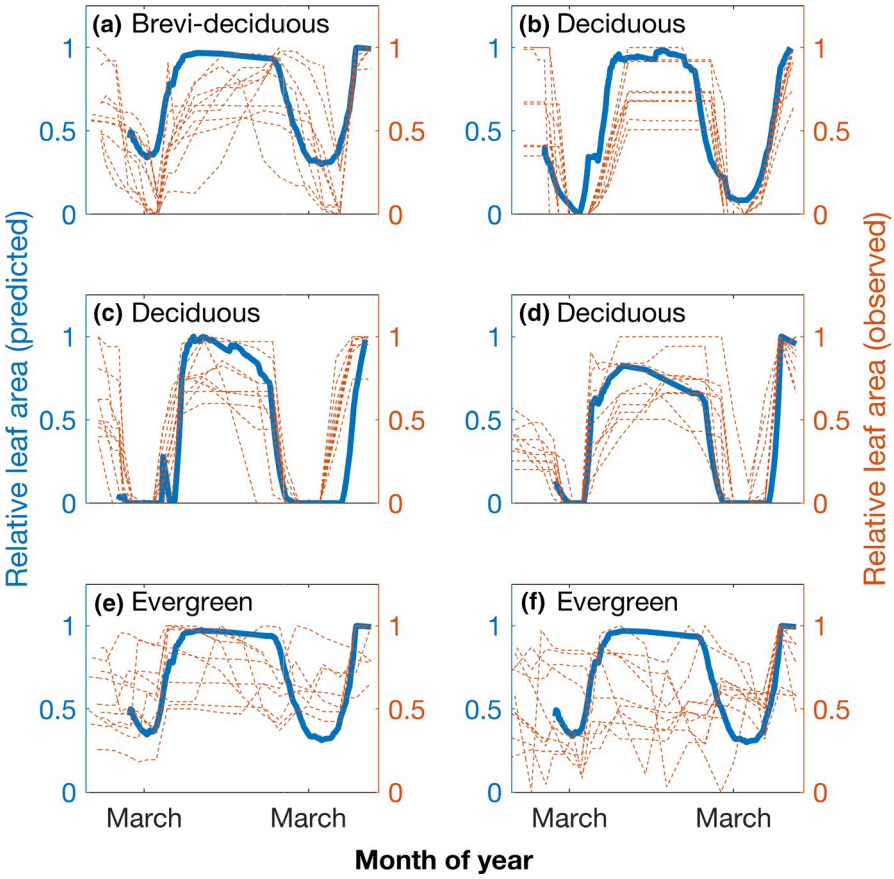

FIGURE 2 Seasonal plasticity in structural allocation to leaves for an annual cycle over the years 2011–2013 in the seasonally dry tropical forests in Panama (Wolfe et al., 2016) for six different species with a range of hydraulic traits and allocation strategies including drought deciduous, brevi-deciduous, and evergreen. HOTTER model predictions (blue) compared to phenology for individual trees (red lines). Tree species include: (a) *Annona hayesii* (brevi-deciduous), (b) *Genipa americana* (deciduous), (c) *Bursera simaruba* (deciduous), (d) *Cavanillesia platanifolia* (deciduous), (e) *Cojoba rufescens* (evergreen), (f) *Astronium graveolens* (evergreen)

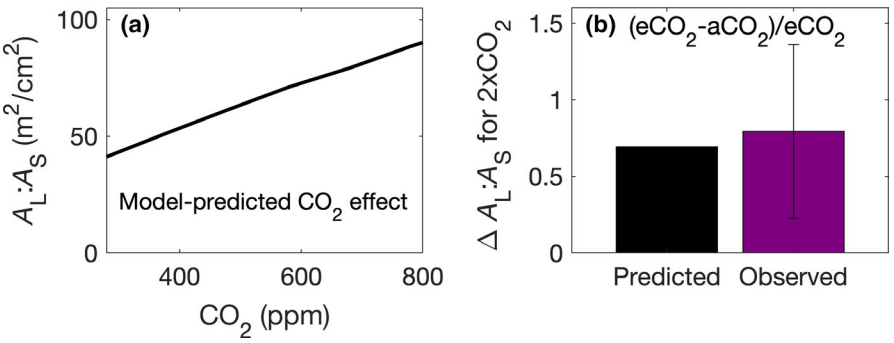

FIGURE 3 Model-predicted optimal allocation to leaf area relative to sapwood area (A_L:A_S) and meta-analysis predicted A_L:A_S responses across atmospheric CO_2 gradients. (a) Model-predicted optimal A_L:A_S response to atmospheric CO_2 concentrations ranging from preindustrial levels to an approximate doubling of current CO_2 concentrations. (b) Predicted fractional change in A_L:A_S (i.e., (eCO_2 − aCO_2)/(aCO_2)) for a doubling of atmospheric CO_2 concentrations from 400 to 800 ppm using the HOTTER model (black) and mixed effects model coefficients derived from meta-analysis–observed CO_2 fertilization responses (purple). Error bars represent 95% confidence intervals for mixed effects model coefficient

South America due to the large predicted increase in VPD in a region comprised predominantly of wet-adapted species (Figures 4c and 5).

Of the traits tested, A_L:A_S responses were most sensitive to plant hydraulic traits. Compared to traits including SLA, $V_{c,max}$, and K_{max}, interspecific variation in P50 resulted in the largest change in allocation strategy to A_L:A_S between predictions where P50 was held at a constant global mean value (Materials and Methods) versus predictions where P50 varied by biome and vegetation type (Figure 5). The P50 effect was strongest in wet tropical forests where model predictions with a constant P50 predicted a much larger A_L:A_S compared to the predictions with biome-specific traits due to an underestimation of the hydraulic vulnerability of moist tropical forests in the fixed trait scenario.

4 | DISCUSSION

This study combines multiple observational datasets of leaf area adjustment along temporal and spatial environmental gradients

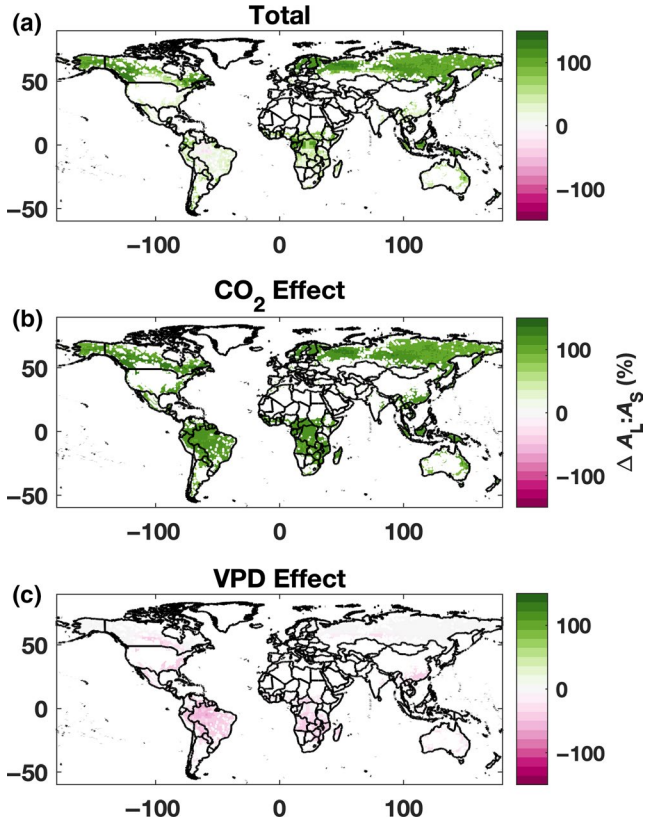

FIGURE 4 (a) Projected percentage change in canopy leaf area relative to tree sapwood area (A_L:A_S) for the 2080–2099 climatological mean relative to 1981–2000. (b) Projected percentage change in canopy leaf area relative to tree sapwood area due to CO_2 fertilization alone. (c) Projected percentage change in canopy leaf area relative to tree sapwood area due to increased vapor pressure deficit (VPD) alone

in diverse biomes, a meta-analysis of the CO_2 fertilization effects on leaf area, and a tractable, rigorous model of optimal plant carbon allocation based on known physiological mechanisms of hydraulic gas exchange coupling. We find strong evidence that observed allocation strategies to leaf area over time and space and across multiple biomes can be explained by our optimality approach. With projected increases of atmospheric CO_2 and VPD, our optimality approach suggests that, for mean conditions, increased water use efficiency associated with increasing atmospheric CO_2 concentrations overcompensates for increased water stress associated with higher atmospheric VPD, potentially driving increases in leaf area globally. Exceptions include parts of wet tropical forests where strong VPD stress combined with wet-adapted plant hydraulic trait strategies inhibits increases in A_L:A_S. From a theoretical/first principles perspective, the moderating effect that increased atmospheric CO_2 concentrations have on maintaining or increasing A_L:A_S in spite of increased VPD are not unexpected because increased atmospheric CO_2 increases plant water use efficiency and decrease water demand per unit leaf area, so there is significant potential for trees to support a greater leaf area with less sapwood area, even with substantial temperature-driven increases in atmospheric VPD.

By evaluating the sensitivity of these allocation trends to other plant traits, we find that hydraulic traits in particular have an enormous impact on modeled forest leaf area globally. Given that allocation strategy to A_L:A_S is most sensitive to plant hydraulic traits, and hydraulic traits have been shown to be critical in explaining both tree productivity and mortality responses during drought (Anderegg et al., 2016, 2018), these results further emphasize the importance of simulating A_L:A_S not as a fixed allometric trait in large-scale vegetation models, but rather as an adaptive property of plant traits and environment.

A potentially moderating factor to the predicted increase in A_L:A_S is increased light limitation with growth (Luo et al., 2004), a process which is not currently included in HOTTER. Specifically, if vegetation productivity and leaf area index (LAI) increases, more competition for light could lead to more allocation to stems to outgrow neighboring competitors, particularly in light-limited regions such as the tropics. Furthermore, competition for water and nutrients may stimulate increased root allocation relative to leaves. Although HOTTER did not explain the lack of intra-annual variation in A_L:A_S in the tropical dry forest evergreen species (Figure 2e,f), HOTTER predicted that the more resistant xylem found in the evergreen species (realized through xylem vulnerability curves in the model) supplied sufficient water to the tree crown to merit some leaf retention during the dry season. In the observations, the absence of any leaf shedding in the evergreen trees likely reflects a strategy that capitalizes on lower competition for light during the dry season (Detto, Wright, Calderón, & Muller-Landau, 2018; Wright & van Schaik, 1994), and the additional nutrient and carbon constraints associated with growing new leaves on an annual basis. Given that light competition and nutrient constraints are not processes directly incorporated in the HOTTER model (see Materials and Methods), it is not surprising that HOTTER did a poor job predicting seasonal variations in evergreen A_L:A_S. However, these results highlight that plant hydraulic traits are critical to the tropical dry forest evergreen tree strategy that capitalizes on dry season productivity.

Finally, additional experimental studies targeting CO_2-driven changes in A_L:A_S and the scaling of A_L:A_S from branch to tree to ecosystem are needed to refine our understanding of tree structural allocation strategies. Despite these caveats, the insights from HOTTER scale tissue-level properties to tree-level photosynthetic responses and trade-offs, providing an important mechanistic foundation to understanding how plant traits and environment jointly constrain carbon allocation strategy.

The predicted allocational sensitivity, A_L:A_S, due to changes in mean climate and increased atmospheric CO_2 has important implications for forest productivity. Specifically, fixed allocation strategies used in many vegetation models that are independent of climate (De Kauwe et al., 2014) would tend to underestimate both future productivity (through suboptimal allocation to A_L:A_S, e.g., Figure S1), and potentially ecosystem vulnerability to catastrophic mortality events. While it is unclear how these two compensating processes will interact to influence the accuracy of the magnitude

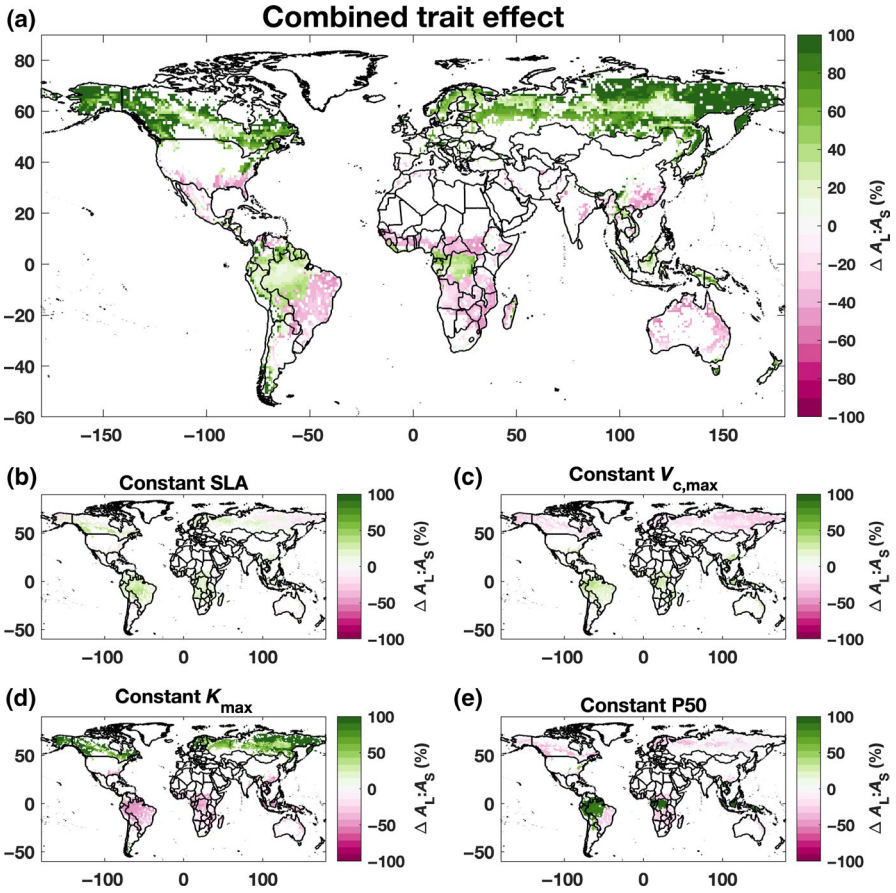

FIGURE 5 Effects of biome-specific traits including specific leaf area (SLA), maximum rate of carboxylation ($V_{c,max}$), maximum stem water conductivity (K_{max}), and the water potential at which 50% loss of stem hydraulic conductance occurs (P50) on A_L:A_S predictions. (a) Projected percentage change in A_L:A_S for globally constant SLA, $V_{c,max}$, K_{max}, and P50 relative to globally varying SLA, $V_{c,max}$, K_{max}, and P50. (b) Projected percentage change in A_L:A_S for globally constant SLA only relative to globally varying traits. (c) Projected percentage change in A_L:A_S for $V_{c,max}$ only relative to globally varying traits. (d) Projected percentage change in A_L:A_S for globally constant K_{max} only relative to globally varying traits. (e) Projected percentage change in A_L:A_S for globally constant P50 only relative to globally varying traits

and sign of projections for the terrestrial carbon sink, it is clear that hydraulic constraints are a fundamental process governing plant carbon allocation strategy (Figures 1 and 5), productivity (Anderegg et al., 2018), and mortality (Jump et al., 2017; Trugman et al., 2018).

Here, we explicitly couple plant hydraulics with carbon metabolism to demonstrate that hydraulic functional traits and environment are prognostic of tree carbon allocation strategy. Given that vegetation models are now largely functional trait based (Fisher et al., 2018), and substantial advances in vegetation models are being made so that now many regional-scale models resolve plant hydraulics (Kennedy et al., 2019; Xu, Medvigy, Powers, Becknell, & Guan, 2016), it is timely and feasible to implement dynamic carbon allocation schemes into these models. Our optimization-based model provides the mechanistic underpinning motivating (a) explicit representation of plant hydraulics in vegetation models and (b) the representation of allocation to A_L:A_S as an emergent property of environment and plant hydraulic traits.

ACKNOWLEDGEMENTS

We acknowledge the World Climate Research Programme's Working Group on Coupled Modelling, which is responsible for CMIP, and we thank the climate modeling groups (listed in the Supplementary Information) for producing and making available their model output. A.T.T. acknowledges support from the USDA National Institute of Food and Agriculture Postdoctoral Research Fellowship Grant No. 2018-67012-28020. W.R.L.A. acknowledges funding from the David and Lucille Packard Foundation, University of Utah Global Change and Sustainability Center, NSF Grants 1714972 and 1802880, and the USDA National Institute of Food and Agriculture, Agricultural and Food Research Initiative Competitive Programme, Ecosystem Services and Agro-ecosystem Management, grant no. 2018-67019-27850. B.T.W. was supported by the Next-Generation Ecosystem Experiments-Tropics, funded by the U.S. Department of Energy, Office of Science, Biological and Environmental Research. N.K.R. was supported in part by the German Federal Ministry of Education and Research (BMBF), through the Helmholtz Association and its research program ATMO, and by the German Research Foundation through its Emmy Noether Program grant no. RU 1657/2-1. B.B. received funding from the German Research Foundation through its German-Israeli project cooperation program grant no. YA 274/1-1 and SCHM 2736/2-1. All CMIP5 multimodel ensemble data are available at the Centre for Environmental Data Archival (https://services.ceda.ac.uk/).

CONFLICT OF INTEREST

The authors declare no conflict of interest.

ORCID

Anna T. Trugman https://orcid.org/0000-0002-7903-9711
William R. L. Anderegg https://orcid.org/0000-0001-6551-3331

REFERENCES

Ainsworth, E. A., & Long, S. P. (2005). What have we learned from 15 years of free-air CO_2 enrichment (FACE)? A meta-analytic review of the responses of photosynthesis, canopy properties and plant production to rising CO_2. *New Phytologist*, *165*(2), 351–371. https://doi.org/10.1111/j.1469-8137.2004.01224.x

Anderegg, W. R. L. (2015). Spatial and temporal variation in plant hydraulic traits and their relevance for climate change impacts on vegetation. *New Phytologist*, 1008–1014. https://doi.org/10.1111/nph.12907

Anderegg, W. R., Klein, T., Bartlett, M., Sack, L., Pellegrini, A. F., Choat, B., & Jansen, S. (2016). Meta-analysis reveals that hydraulic traits explain cross-species patterns of drought-induced tree mortality across the globe. *Proceedings of the National Academy of Sciences of the United States of America*, *113*(18), 5024–5029. https://doi.org/10.5061/dryad.116j2

Anderegg, W. R. L., Konings, A. G., Trugman, A. T., Yu, K., Bowling, D. R., Gabbitas, R., … Zenes, N. (2018). Hydraulic diversity of forests regulates ecosystem resilience during drought. *Nature*, *561*, 538–541. https://doi.org/10.1038/s41586-018-0539-7

Baldocchi, D. D., & Xu, L. (2007). What limits evaporation from Mediterranean oak woodlands – The supply of moisture in the soil, physiological control by plants or the demand by the atmosphere? *Advances in Water Resources*, *30*(10), 2113–2122. https://doi.org/10.1016/j.advwatres.2006.06.013

Carter, J. L., & White, D. A. (2009). Plasticity in the Huber value contributes to homeostasis in leaf water relations of a mallee Eucalypt with variation to groundwater depth. *Tree Physiology*, *29*(11), 1407–1418. https://doi.org/10.1093/treephys/tpp076

Channan, S., Collins, K., & Emanuel, W. R. (2014). Global mosaics of the standard MODIS land cover type data. *University of Maryland and the Pacific Northwest National Laboratory, College Park, Maryland, USA*.

De Kauwe, M. G., Medlyn, B. E., Zaehle, S., Walker, A. P., Dietze, M. C., Wang, Y. P., … Norby, R. J. (2014). Where does the carbon go? A model-data intercomparison of vegetation carbon allocation and turnover processes at two temperate forest free-air CO_2 enrichment sites. *New Phytologist*, *203*(3), 883–899. https://doi.org/10.1111/nph.12847

DeLucia, E. H., Maherali, H., & Carey, E. V. (2000). Climate-driven changes in biomass allocation in pines. *Global Change Biology*, *6*(5), 587–593. https://doi.org/10.1046/j.1365-2486.2000.00338.x

Detto, M., Wright, S. J., Calderón, O., & Muller-Landau, H. C. (2018). Resource acquisition and reproductive strategies of tropical forest in response to the El Niño-Southern Oscillation. *Nature Communications*, *9*(1), 1–8. https://doi.org/10.1038/s41467-018-03306-9

Eagleson, P. S. (1982). Ecological optimality in water-limited natural soil-vegetation systems: 1. Theory and hypothesis. *Water Resources Research*, *18*(2), 325–340. https://doi.org/10.1029/WR018i002p00325

Farquhar, G. D., Caemmerer, S., & Berry, J. A. (1980). A biochemical model of photosynthetic CO_2 assimilation in leaves of C3 species. *Planta*, *149*, 78–90. https://doi.org/10.1007/BF00386231

Fick, S. E., & Hijmans, R. J. (2017). WorldClim 2: New 1-km spatial resolution climate surfaces for global land areas. *International Journal of Climatology*, *37*(12), 4302–4315. https://doi.org/10.1002/joc.5086

Fisher, R. A., Koven, C. D., Anderegg, W. R. L., Christoffersen, B. O., Dietze, M. C., Farrior, C. E., … Moorcroft, P. R. (2018). Vegetation demographics in Earth System Models: A review of progress and priorities. *Global Change Biology*, *24*(1), 35–54. https://doi.org/10.1111/gcb.13910

Franklin, O., Johansson, J., Dewar, R. C., Dieckmann, U., McMurtrie, R. E., Brännström, A. K., & Dybzinski, R. (2012). Modeling carbon allocation in trees: A search for principles. *Tree Physiology*, *32*(6), 648–666. https://doi.org/10.1093/treephys/tpr138

Friedl, M. A., Sulla-Menashe, D., Tan, B., Schneider, A., Ramankutty, N., Sibley, A., & Huang, X. (2010). MODIS Collection 5 global land cover: Algorithm refinements and characterization of new datasets, 2001-2012. *Collection 5.1 IGBP Land Cover, Boston University, Boston, MA, USA*.

Gholz, H. L. (1982). Environmental limits on aboveground net primary production, leaf area, and biomass in vegetation zones of the Pacific Northwest. *Ecology*, *63*(2), 469–481. https://doi.org/10.2307/1938964

Gielen, B., & Ceulemans, R. (2001). The likely impact of rising atmospheric CO_2 on natural and managed Populus: A literature review. *Environmental Pollution*, *115*, 335–358. https://doi.org/10.1016/S0269-7491(01)00226-3

Huang, C., Domec, J., Ward, E. J., Duman, T., Manoli, G., Parolari, A. J., & Katul, G. G. (2017). The effect of plant water storage on water fluxes within the coupled soil–plant system. *New Phytologist*, *213*, 1093–1106. https://doi.org/10.1111/nph.14273

Hubbard, R. M., Ryan, M. G., Stiller, V., & Sperry, J. S. (2001). Stomatal conductance and photosynthesis vary linearly with plant hydraulic conductance in ponderosa pine. *Plant, Cell and Environment*, *24*, 113–121. https://doi.org/10.1046/j.1365-3040.2001.00660.x

Joffre, R., & Ramball, S. (1993). How tree cover influences the water balance of Mediterranean rangelands. *Ecology*, *74*(2), 570–582. https://doi.org/10.2307/1939317

Jump, A. S., Ruiz-Benito, P., Greenwood, S., Allen, C. D., Kitzberger, T., Fensham, R., … Lloret, F. (2017). Structural overshoot of tree growth with climate variability and the global spectrum of drought-induced forest dieback. *Global Change Biology*, *23*(9), 3742–3757. https://doi.org/10.1111/gcb.13636

Kennedy, D., Swenson, S., Oleson, K. W., Lawrence, D. M., Fisher, R. A., da Costa, A. C. L., & Gentine, P. (2019). Implementing plant hydraulics in the Community Land Model, version 5. *Journal of Advances in Modeling Earth Systems*, *11*, 485–513. https://doi.org/10.1029/2018ms001500

Leuning, R. (1995). A critical appraisal of combined stomatal-photosynthesis model for C3 plants. *Plant, Cell and Environment*, *18*, 339–355. https://doi.org/10.1111/j.1365-3040.1995.tb00370.x

Limousin, J.-M., Rambal, S., Ourcival, J.-M., Rodríguez-Calcerrada, J., Pérez-Ramos, I. M., Rodríguez-Cortina, R., … Joffre, R. (2012). Morphological and phenological shoot plasticity in a Mediterranean evergreen oak facing long-term increased drought. *Oecologia*, *169*, 565–577. https://doi.org/10.1007/s00442-011-2221-8

Luo, Y., Su, B., Currie, W. S., Dukes, J. S., Finzi, A., Hartwig, U., … Field, C. B. (2004). Progressive nitrogen limitation of ecosystem responses to rising atmospheric carbon dioxide. *BioScience*, *54*(8), 731. https://doi.org/10.1641/0006-3568(2004) 054[0731:PNLOER]2.0.CO;2

Mäkelä, A., & Valentine, H. T. (2001). The ratio of NPP to GPP: Evidence of change over the course of stand development. *Tree Physiology*, *21*, 1015–1030. https://doi.org/10.1093/treephys/21.14.1015

Martínez-Vilalta, J., Cochard, H., Mencuccini, M., Sterck, F., Herrero, A., Korhonen, J. F. J., … Zweifel, R. (2009). Hydraulic adjustment of Scots pine across Europe. *New Phytologist*, *184*, 353–364. https://doi.org/10.1111/j.1469-8137.2009.02954.x

Medvigy, D., Wofsy, S. C., Munger, J. W., Hollinger, D. Y., & Moorcroft, P. R. (2009). Mechanistic scaling of ecosystem function and dynamics in space and time: Ecosystem demography model version 2. *Journal of Geophysical Research*, *114*(G1), G01002. https://doi.org/10.1029/2008JG000812

Meinzer, F. C., Goldstein, G., & Andrade, J. L. (2001). Regulation of water flux through tropical forest canopy trees: Do universal rules apply? *Tree Physiology*, *21*, 19–26. https://doi.org/10.1093/treephys/21.1.19

Mencuccini, M., & Bonosi, L. (2001). Leaf/sapwood area ratios in Scots pine show acclimation across Europe. *Canadian Journal of Forest Research*, *31*(3), 442–456. https://doi.org/10.1139/x00-173

Mencuccini, M., & Grace, J. (1994). Climate influences the leaf area/sapwood area in scots pine. *Tree Physiology*, *15*(2), 1–10. https://doi.org/10.1093/treephys/15.1.1

Mencuccini, M., Manzoni, S., & Christoffersen, B. O. (2018). Modelling water fluxes in plants: From tissues to biosphere and back. *New Phytologist*, *1991*, 1–24. https://doi.org/10.1111/nph.15681

Myneni, R., Dong, J., Tucker, C. J., Kaufmann, P. E., Kauppi, P. E., Liski, J., … Hughes, M. K. (2001). A large carbon sink in the woody biomass of Northern forests. *Proceedings of the National Academy of Sciences of the United States of America*, *98*, 14784–14789. https://doi.org/10.1073/pnas.261

Nemani, R. R., Keeling, C. D., Hashimoto, H., Jolly, W. M., Piper, S. C., Tucker, C. J., & Running, S. W. (2003). Climate-driven increases in global terrestrial net primary production from 1982 to 1999. *Science*, *300*(June), 1560–1564. https://doi.org/10.1126/science.1082750

Novick, K. A., Ficklin, D. L., Stoy, P. C., Williams, C. A., Bohrer, G., Oishi, A. C., … Phillips, R. P. (2016). The increasing importance of atmospheric demand for ecosystem water and carbon fluxes. *Nature Climate Change*, *6*, 1023–1027. https://doi.org/10.1038/nclimate3114

Oleson, K. W., Lawrence, D. M., Bonan, G. B., Flanner, M. G., Kluzek, E., Lawrence, P. J., … Thornton, P. E. (2010). Technical description of version 4.0 of the Community Land Model (CLM). *NCAR Technical Notes*, TN-478, 1–257.

Park Williams, A., Allen, C. D., Macalady, A. K., Griffin, D., Woodhouse, C. A., Meko, D. M., … McDowell, N. G. (2012). Temperature as a potent driver of regional forest drought stress and tree mortality. *Nature Climate Change*, *3*(3), 292–297. https://doi.org/10.1038/nclimate1693

Pinol, J., & Sala, A. (2000). Ecological implications of xylem cavitation for several Pinaceae in the Pacific Northern USA. *Functional Ecology*, *14*(5), 538–545. https://doi.org/10.1046/j.1365-2435.2000.00451.x

Rosas, T., Mencuccini, M., Barba, J., Cochard, H., Saura-Mas, S., & Martínez-Vilalta, J. (2019). Adjustments and coordination of hydraulic, leaf and stem traits along a water availability gradient. *New Phytologist*, https://doi.org/10.1111/nph.15684

Shinozaki, K., Yoda, K., Hozumi, K., & Kira, T. (1964). A quantitative analysis of plant form – The pipe model theory: I. Basic analyses. *Japanese Journal of Ecology*, *14*(3), 97–105. https://doi.org/10.18960/seitai.14.3_97

Simard, M., Pinto, N., Fisher, J. B., & Baccini, A. (2011). Mapping forest canopy height globally with spaceborne lidar. *Journal of Geophysical Research*, *116*(G4). https://doi.org/10.1029/2011jg001708

Smith, N. G., Keenan, T. F., Colin Prentice, I., Wang, H., Wright, I. J., Niinemets, Ü., … Zhou, S.-X. (2019). Global photosynthetic capacity is optimized to the environment. *Ecology Letters*, *22*, 506–517. https://doi.org/10.1111/ele.13210

Sperry, J. S. (2000). Hydraulic constraints on plant gas exchange. *Agricultural and Forest Meteorology*, *104*(1), 13–23. https://doi.org/10.1016/S0168-1923(00)00144-1

Sperry, J. S., Adler, F. R., Campbell, G. S., & Comstock, J. P. (1998). Limitation of plant water use by rhizosphere and xylem conductance: Results from a model. *Plant, Cell and Environment*, *21*, 347–359. https://doi.org/10.1046/j.1365-3040.1998.00287.x

Sperry, J. S., & Love, D. M. (2015). What plant hydraulics can tell us about responses to climate-change droughts. *New Phytologist*, *207*(1), 14–27. https://doi.org/10.1111/nph.13354

Trugman, A. T., Detto, M., Bartlett, M. K., Medvigy, D., Anderegg, W. R. L., Schwalm, C., … Pacala, S. W. (2018). Tree carbon allocation explains forest drought-kill and recovery patterns. *Ecology Letters*, *21*(10), 1552–1560. https://doi.org/10.1111/ele.13136

Wang, H., Prentice, I. C., Keenan, T. F., Davis, T. W., Wright, I. J., Cornwell, W. K., … Peng, C. (2017). Towards a universal model for carbon dioxide uptake by plants. *Nature Plants*, *3*(9), 734–741. https://doi.org/10.1038/s41477-017-0006-8

Wolf, A., Anderegg, W. R., & Pacala, S. W. (2016). Optimal stomatal behavior with competition for water and risk of hydraulic impairment. *Proceedings of the National Academy of Sciences of the United States of America*, *113*(46), E7222–E7230. https://doi.org/10.1073/pnas.1615144113

Wolfe, B. T., & Goldstein, G. (2017). Retention of stored water enables tropical tree saplings to survive extreme drought conditions. *Tree Physiology*, *37*(4), 469–480. https://doi.org/10.1093/treephys/tpx001

Wolfe, B. T., Sperry, J. S., & Kursar, T. A. (2016). Does leaf shedding protect stems from cavitation during seasonal droughts? A test of the hydraulic fuse hypothesis. *New Phytologist*, *212*(4), 1007–1018. https://doi.org/10.1111/nph.14087

Wright, S. J., & van Schaik, C. P. (1994). Light and the phenology of tropical trees. *The American Naturalist*, *143*(1), 192–199. https://doi.org/10.1086/285600

Xu, X., Medvigy, D., Powers, J. S., Becknell, J. M., & Guan, K. (2016). Diversity in plant hydraulic traits explains seasonal and inter-annual variations of vegetation dynamics in seasonally dry tropical forests. *New Phytologist*, https://doi.org/10.1111/nph.14009

Zhu, Z., Piao, S., Myneni, R. B., Huang, M., Zeng, Z., Canadell, J. G., … Zeng, N. (2016). Greening of the Earth and its drivers. *Nature Climate Change*, *6*, 791–796. https://doi.org/10.1038/NCLIMATE3004

SUPPORTING INFORMATION

Additional supporting information may be found online in the Supporting Information section at the end of the article.

How to cite this article: Trugman AT, Anderegg LDL, Wolfe BT, et al. Climate and plant trait strategies determine tree carbon allocation to leaves and mediate future forest productivity. *Glob Change Biol*. 2019;00:1–11. https://doi.org/10.1111/gcb.14680